Short communication

External sensory-motor cues while managing unexpected slippages can violate the planar covariation law

F. Aprigliano [a,1], V. Monaco [a,b,*,1], S. Micera [a,c]

[a] The BioRobotics Institute, Scuola Superiore Sant'Anna, Pisa, Italy
[b] IRCCS Fondazione Don Carlo Gnocchi, Milan, Italy
[c] Bertarelli Foundation Chair in Translational NeuroEngineering, Center for Neuroprosthetics and Institute of Bioengineering, School of Engineering, Ecole Polytechnique Federale de Lausanne, Lausanne, Switzerland

ABSTRACT

This study was aimed at investigating the intersegmental coordination of six older adults while managing unexpected slippages delivered during steady walking, and wearing an Active Pelvis Orthosis (APO). The APO was setup either to assist volunteers at the hip levels during balance loss or to be transparent. The Planar Covariation Law (PCL) of the lower limb elevation angles was the main tool used to assess the intersegmental coordination of both limbs (i.e., the perturbed and unperturbed ones). Results revealed that, after the onset of the perturbation, elevation angles of both limbs do not covary, a part from the robot-mediated assistance. These new evidences suggest that external sensory-motor cues can alter the temporal synchronization of elevation angles, thus violating the PCL.

1. Introduction

The Planar Covariation Law (PCL) has been widely used to describe the relationship among lower limb segments during locomotion-related motor tasks (Borghese et al., 1996; Ivanenko et al., 2008; Lacquaniti et al., 2002). Specifically, according to the PCL, elevation angles of lower limb segments covary despite leg joint angles are significantly altered by the motor tasks being achieved (Ivanenko et al., 2007).

Recent findings further extended this notion, revealing that the PCL can be considered a control strategy shared across volitional and likely involuntary motor behaviors, and seems to reflect the relationship between intersegmental coordination and control of the dynamic balance in humans (Aprigliano et al., 2017, 2016; Funato et al., 2015).

However, the origin of the PCL is still an open question. Some authors suggested that the PCL mainly reflects a biomechanical constraint, that is, a strong coupling of lower limb segments probably mediated by bi-articular muscle groups (Hicheur, 2006). Others, by using different approaches, corroborated the hypothesis that the control of intersegmental coordination is likely to be func-tional and is expected to have neural origin (Barliya et al., 2009; Funato et al., 2015; Ivanenko et al., 2008).

In this study we investigated the PCL of lower limb segments while elderly subjects were managing unexpected slippages assisted by an Active Pelvis Orthosis (APO) in order to add further insights concerning the physiological meaning of the PCL.

2. Methods

2.1. Experimental setup and protocol

A subset of data used in this study was collected for an independent work (Monaco et al., 2017). Six healthy elders (six males, 68.1 ± 4.8 years old, 77.1 ± 7.8 kg, 1.75 ± 0.7 m) were enrolled after providing informed consent. Research procedures complied with the Declaration of Helsinki and were approved by the Institutional Ethics Committee (Don Gnocchi Foundation, Florence, Italy).

Participants were asked to manage unexpected slippages delivered while steadily walking at their preferred speed (0.91 ± 0.14 m/s). Perturbations were provided by a custom made split-belts treadmill ((Bassi Luciani et al., 2012), Fig. 1A) and consisted of a sudden forward movement of the right belt triggered by the heel strike of the right foot (belts velocity profiles are shown in Fig. 1C). Subjects donned a safety harness for safety issues.

Participants also wore a powered wearable robot, i.e. APO, designed to assist hip flexion-extension (Fig. 1A). The APO can
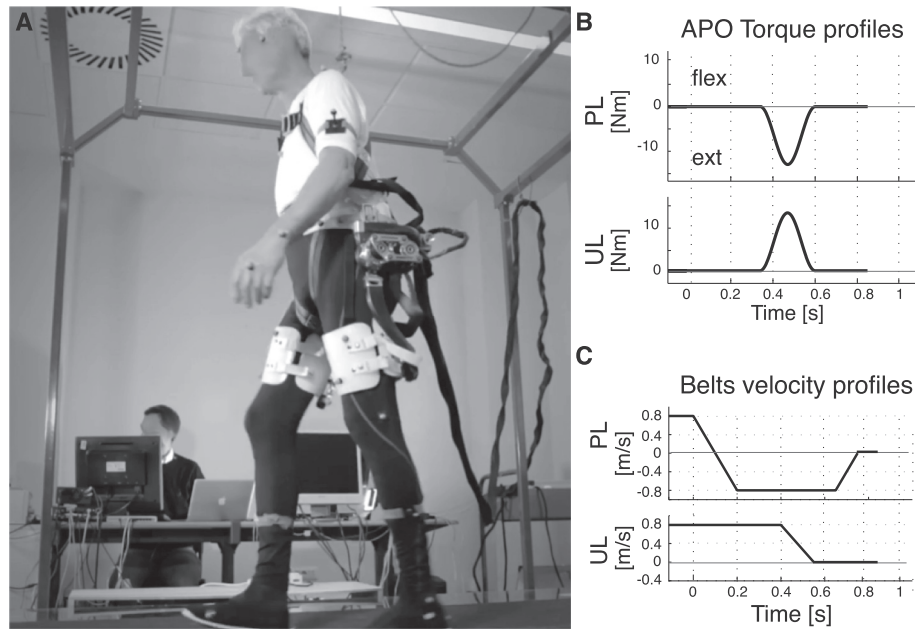

Fig. 1. Experimental setup, speed profiles, and torques supplied by the Active Pelvis Orthosis (APO). (A) The mechatronic platform delivers unexpected slippage while the subject is wearing the APO and steadily walking on the treadmill. (B) Representative APO torque profiles applied to the perturbed and unperturbed limb (PL and UL).(C) Representative belts velocity profiles for the PL and UL. In panels B and C, 0 represents the onset of the perturbation.

actively assist hip flexion-extension, and is endowed with two free rotational degree of freedom for hip abduction-adduction. More details can be found elsewhere (Giovacchini et al., 2015).

The working-modality of the APO can switch between: (i) Z-mode (zero-torque mode), designed to be compliant to the user's intention (Martelli et al., 2014); (ii) A-mode (assistive mode), that is always transparent until balance loss is detected by a detection algorithm running in the APO control unit (Tropea et al., 2015). In this latter case, the robot supplies assistive torques at both hip joints aimed at simultaneously extending the perturbed limb (PL) and flexing the unperturbed one (UL; Fig. 1B).

The protocol consisted of two repetitions for each of the robot working-modalities (i.e., A- and Z- modes), and three additional trials where no perturbation was delivered. All trials were randomly arranged to reduce the effect of the adaptation.

With respect to the purpose of this study, we retained the 3D trajectory of a subset of the whole marker set considering those located on the lower limbs. Kinematics records, belts movements and the APO were synchronized by means of a logic pulse generated by split-belt treadmill during the delivery of the perturbations.

2.2. Data analyses

Raw data were firstly pre-process to remove effects of noise. Touch down and lift off were identified by visual inspection of feet kinematics.

Data were subdivided in two time-windows (Fig. 2): (i) unperturbed stride, starting with the right heel strike before the perturbation onset and ending at the heel strike triggering the perturbation; (ii) compensatory stride, starting simultaneously with the end of the previous stride and ending with the following ipsilateral heel strike. The duration of both unperturbed and compensatory strides were calculated.

The elevation angles of thigh, shank and foot were estimated for both limbs under the hypothesis of planar movement (Ivanenko et al., 2007), and for both strides across the perturbation onset. The range of motion for all elevation angles (RoM_T, RoM_S, RoM_F)
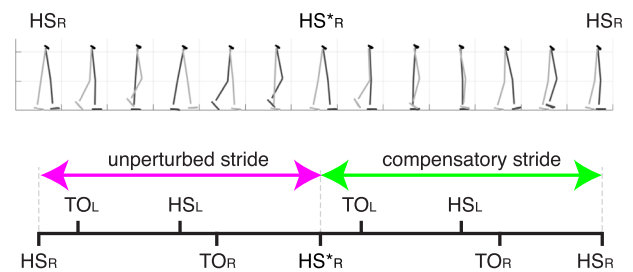

Fig. 2. Time windows across the perturbation onset (HS_R^*). Stick diagram considering the unperturbed and compensatory strides; dark and light grey lines refer to PL and UL, respectively. Heel strike and toe off are shown for the right (HS_R and TO_R) and left foot (HS_L and TO_L), before and after the perturbation onset. Phases of the gait cycle during unperturbed and compensatory strides are reported in magenta and green lines, respectively. (For interpretation of the references to colour in this figure legend, the reader is referred to the web version of this article.)

was computed as the difference between the maximum and the minimum values during unperturbed and compensatory strides.

The principal component analysis (PCA) was performed on standardized (zero mean and unit variance) elevation angles (Aprigliano et al., 2017, 2016) to investigate the PCL during unperturbed and compensatory strides and while the APO was working in Z- and A-mode. We assumed that elevation angles would lie on a plane if the cumulative explained variance (CEV%), accounted for by the first two principal components, was >99% (Borghese et al., 1996; Courtine, 2004). The misalignment between covariation planes pertaining to unperturbed and compensatory strides was estimated by means of the dot product between their related orthogonal vectors (i.e., third eigenvectors of the related covariance matrices), named dot_{w3}. Two covariation planes were considered coinciding if dot_{w3} was higher than 0.99 (Aprigliano et al., 2016).

2.3. Statistical analysis

Outcome variables (strides duration, RoM, CEV% and dot_{w3}) were used as dependent measures.

Table 1
Range of motion of thigh, shank and foot elevation angles (RoM$_T$, RoM$_S$ and RoM$_F$, respectively) are reported for both limbs (PL and UL), before (PRE) and after the perturbation onset, while the APO was working in A- and Z-modes (mean ± 1 standard deviation).

Variable	Limb	PRE	POST	
			A-mode	Z-mode
RoM$_T$	PL	35.9 ± 7.2	32.3 ± 5.0	36.1 ± 7.8
	UL	32.2 ± 4.4	32.3 ± 3.9	32.1 ± 3.9
RoM$_S$	PL	58.5 ± 7.4	33.9 ± 12.2	32.2 ± 9.6
	UL	58.1 ± 7.8	43.7 ± 8.0	44.2 ± 9.0
RoM$_F$	PL	66.3 ± 10.3	31.0 ± 7.3	31.6 ± 11.1
	UL	63.8 ± 11.9	51.1 ± 9.2	55.8 ± 13.4

Table 2
2-way ANOVA performed on RoM$_T$, RoM$_S$ and RoM$_F$ related to data$_{POST}$. Main effect of the exoskeleton working-modalities (i.e., A- and Z-mode; p$_{exos}$) and the limb (i.e., PL and UL; p$_{limb}$), and their interaction (p$_{exos*limb}$) were reported while the subjects were managing AP slippages.

Variable	p$_{exos}$	p$_{limb}$	p$_{exos*limb}$
RoM$_T$	0.056	0.115	0.112
RoM$_S$	0.588	**<0.0001**	0.601
RoM$_F$	0.140	**<0.0001**	0.391

Data reported in bold are statistically significant (p < 0.05).

A t-test for paired samples was used to investigate whether the strides duration was affected by the perturbation (PRE and POST). The same test was performed on data$_{POST}$, to investigate the effect of the exoskeleton working-modalities (A- and Z-modes) on the stride duration.

A 2-way repeated measures ANOVA was performed on RoM, CEV% and dot$_{w3}$: (i) on both the unperturbed and compensatory strides to determine the main and simple interaction effects of perturbation (two levels: PRE and POST) and the observed limb (two levels: UL and PL); and (ii) on data recorded after the perturbation onset (data$_{POST}$), to determine the main and simple interaction effects of the observed limb (two levels: UL and PL) and the exoskeleton working-modality (two levels: A- and Z-mode). The one-sample t-test was used to verify whether the CEV% and the dot$_{w3}$ were lower than the adopted thresholds (i.e., 99% and 0.99, respectively). Statistical significance was set at p < 0.05.

3. Results

3.1. Temporal and kinematic parameters

The compensatory stride duration was significantly (p < 0.001) shortened (0.79 ± 0.19 s) than that referring to steady locomotion (1.02 ± 0.14 s). After the perturbation, no difference about the stride duration was observed between the exoskeleton-working modalities (p > 0.05).

The RoM of the elevation angles are reported in Table 1.

The 2-way ANOVA performed on RoM recorded before and after the perturbation onset showed a significant effect of the observed limb (all p-values < 0.003), revealing a different behaviour between PL and UL (Table 1). Concerning only the proximal segments (RoM$_S$ and RoM$_F$), it was noticed: a main effect of the perturbation (p < 0.0001; Table 1), involving lower values during the compensatory stride than during the unperturbed one (Table 2); a significant interaction between perturbation and limb factors (p < 0.001; Table 1).

Considering data$_{POST}$, the analyses highlighted a significant effect of the limb for RoM$_S$ and RoM$_F$ (p > 0.0001; Table 2), revealing lower values for PL than for UL (Table 1). No differences were observed between exoskeleton working-modalities.

3.2. Inter-segmental coordination

The lower limbs inter-segmental coordination was examined by plotting the elevation angles one vs. the others in a 3D-position space graph (Fig. 3), during the strides before and after the perturbation onset while the APO was working in Z- and A-modes.
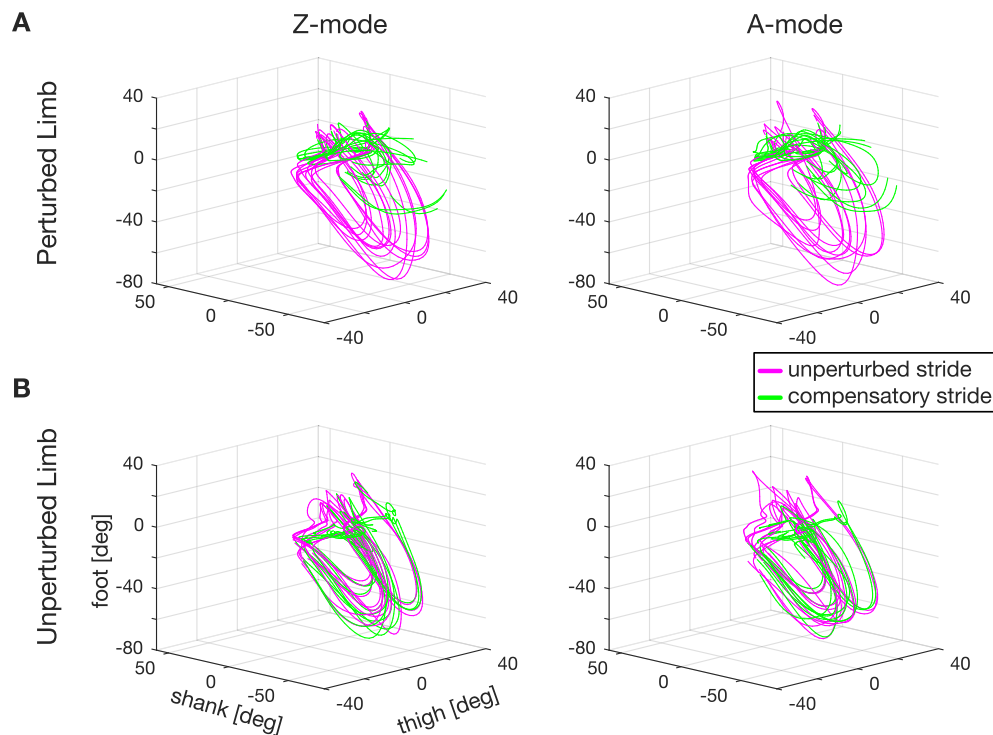

Fig. 3. Planar covariation law of elevation angles at thigh, shank and foot (3D-position space graph). Magenta and green lines showed trajectories obtained before and after the onset of the perturbation, respectively. Results are reported for both PL (A) and UL (B). Trials performed by each subject are superimposed. (For interpretation of the references to colour in this figure legend, the reader is referred to the web version of this article.)

Table 3

CEV% and dot$_{w3}$ are reported, for both limbs (PL and UL), before (PRE) and after the perturbation onset, while the APO was working in A- and Z-modes (mean ± 1 standard deviation). Values that are significantly lower than adopted thresholds are in bold.

Variable	Limb	PRE	POST	
			A-mode	Z-mode
CEV%	PL	99.5 ± 0.01	**98.1 ± 1.0**	**98.1 ± 1.3**
	UL	99.5 ± 0.2	**98.8 ± 0.7**	**98.6 ± 0.6**
dot$_{w3}$	PL	–	**0.95 ± 0.03**	**0.96 ± 0.03**
	UL	–	0.99 ± 0.01	0.99 ± 0.01

Table 4

2-way ANOVA performed on CEV% and dot$_{w3}$ related to data$_{POST}$. Main effect of the exoskeleton working-modalities (i.e., A- and Z-mode; p$_{exos}$) and the limb (i.e., PL and UL; p$_{limb}$), and their interaction (p$_{exos*limb}$) were reported while the subjects were managing AP slippages.

Variable	p$_{exos}$	p$_{limb}$	p$_{exos*limb}$
CEV%	0.892	**0.039**	0.530
dot$_{w3}$	0.559	**<0.0001**	0.629

Data reported in bold are statistically significant (p < 0.05).

The 2-way ANOVA, performed on data recorded before and after the perturbation onset, showed a significant effect of the perturbation (p < 0.0001), revealing that the CEV% extracted during the compensatory stride was significantly lower than those extracted during the unperturbed one (Table 3). In addition, a significant interaction was observed between the perturbation and the limb factors (p = 0.027); no main effect was reported for the limb factor (p = 0.073; Table 3).

Results of the 2-way ANOVA on data$_{POST}$ are reported in Table 4. Analysis of the CEV% showed a significant main effect of the limb, revealing lower values for PL than for UL (Table 3). Noticeably, the CEV%, referred to both limbs, was significantly lower than the adopted threshold (PL: p < 0.0001, UL: p = 0.013; Table 3). Accordingly, during the compensatory stride the PCL was violated for both UL and PL (Fig. 3). Moreover, the CEV% was not affected by the robot working-modalities (A-mode vs Z-mode; Fig. 3, Tables 3 and 4).

Analysis on the orientation of the covariation planes (PRE vs. A-mode; PRE vs. Z-mode), revealed that the dot$_{w3}$ was affected only by the limb factor (Table 4); specifically, it was significantly lower than the adopted threshold (0.99), for the PL (p < 0.0001); and equal to the threshold, for the UL (p > 0.05). Accordingly, planes before and after the perturbations could be considered as congruent only for the UL. No effect of the robot-working modalities was observed (Table 4).

4. Discussion

This study was aimed at investigating the PCL when elders were actively assisted by an APO while managing unexpected slippages. As expected, perturbations reduced stride duration and RoMs of proximal segments (Table 1). In addition, RoMs after the slippage did not change due to the APO working-modes whereas a different behavior between UL and PL was noticed (Tables 1 and 2).

During the compensatory stride, the PCL is violated for the PL (Fig. 3A), apart from the APO working-modalities. This outcome was actually expected and likely reflects the fact that the belt constrains the foot to cover a certain displacement while subjects prevent knee hyperextension (Aprigliano et al., 2017, 2016).

Our analysis also revealed that the PCL of the UL was violated, as well, when the APO was working in both Z-mode (transparent) and A-mode (assistive), that is, elevation angles of the UL did not covary (Fig. 3B), apart from the assistance of the APO. It is worth

noting that the A-mode significantly modifies the reactive behavior of lower limb toward a better balance recovery after a slippage (Monaco et al., 2017). These results suggest that even if the APO is expected to only affect the proximal limb segment (parasitic torque in Z-mode and assistive torque in A-mode; see also (Martelli et al., 2014; Monaco et al., 2017)), it indeed alters the whole intra-limb coordination. In this respect, the contribution of the APO at the hip joint represents a sensory-motor cue that represses the PCL at the UL.

In our opinion, this last result provides further support against the hypothesis raised up by Hicheur and colleagues (Hicheur, 2006), at least with respect to the experimental paradigm adopted in this study. As matter of the facts, these authors hypothesized that the planar covariation of elevation angles arises from a strong coupling between shank and foot segments, with thigh angle independently contributing to the pattern of intersegmental covariation. According to this hypothesis, we would have expected that elevation angles of the UL covaried since the APO only acts on the most proximal limb segment (i.e., elevation angles of shank and foot were supposed not to be influenced by the APO). This was not the case, that is, even if the APO only acts on the thighs, the neuromuscular strategy underlying the control of the UL during a compensatory stride modifies the planar relationship of all elevation angles.

According to these evidences, we can conclude that although the intersegmental coordination law can be elicited by locomotion-related tasks (Ivanenko et al., 2007; Lacquaniti et al., 2002), as well as by perturbations (Aprigliano et al., 2017, 2016; Funato et al., 2015), external sensory-motor cues can alter the temporal synchronization of elevation angles, thus violating the PCL.

Conflict of interest statement

Silvestro Micera is co-founder of and has financial interests in the company IUVO SRL, a spin-off company of Scuola Superiore Sant'Anna aiming at commercially exploiting the APO technology.

Acknowledgments

References

Aprigliano, F., Martelli, D., Micera, S., Monaco, V., 2016. Intersegmental coordination elicited by unexpected multidirectional slipping-like perturbations resembles that adopted during steady locomotion. J. Neurophysiol. 115, 728–740. https://doi.org/10.1152/jn.00327.2015.

Aprigliano, F., Martelli, D., Tropea, P., Pasquini, G., Micera, S., Monaco, V., 2017. Aging does not affect the intralimb coordination elicited by slip-like perturbation of different intensities. J. Neurophysiol. https://doi.org/10.1152/jn.00844.2016.

Barliya, A., Omlor, L., Giese, M.A., Flash, T., 2009. An analytical formulation of the law of intersegmental coordination during human locomotion. Exp. Brain Res. 193, 371–385. https://doi.org/10.1007/s00221-008-1633-0.

Bassi Luciani, L., Genovese, V., Monaco, V., Odetti, L., Cattin, E., Micera, S., 2012. Design and evaluation of a new mechatronic platform for assessment and prevention of fall risks. J. Neuroeng. Rehabil. 9, 51. https://doi.org/10.1186/1743-0003-9-51.

Borghese, N.A., Bianchi, L., Lacquaniti, F., 1996. Kinematic determinants of human locomotion. J. Physiol. 494 (Pt 3), 863–879. https://doi.org/10.1113/jphysiol.1996.sp021539.

Courtine, G., 2004. Tuning of a basic coordination pattern constructs straight-ahead and curved walking in humans. J. Neurophysiol. 91, 1524–1535. https://doi.org/10.1152/jn.00817.2003.

Funato, T., Aoi, S., Tomita, N., Tsuchiya, K., 2015. Validating the feedback control of intersegmental coordination by fluctuation analysis of disturbed walking. Exp. Brain Res. 233, 1421–1432. https://doi.org/10.1007/s00221-015-4216-x.

Giovacchini, F., Vannetti, F., Fantozzi, M., Cempini, M., Cortese, M., Parri, A., Yan, T., Lefeber, D., Vitiello, N., 2015. A light-weight active orthosis for hip movement assistance. Robot. Autonom. Syst., 123–134 https://doi.org/10.1016/j.robot.2014.08.015.

Hicheur, H., 2006. Intersegmental coordination during human locomotion: does planar covariation of elevation angles reflect central constraints? J. Neurophysiol. 96, 1406–1419. https://doi.org/10.1152/jn.00289.2006.

Ivanenko, Y.P., Cappellini, G., Dominici, N., Poppele, R.E., Lacquaniti, F., 2007. Modular control of limb movements during human locomotion. J. Neurosci. 27, 11149–11161. https://doi.org/10.1523/JNEUROSCI.2644-07.2007.

Ivanenko, Y.P., d'Avella, A., Poppele, R.E., Lacquaniti, F., 2008. On the origin of planar covariation of elevation angles during human locomotion. J. Neurophysiol. 99, 1890–1898. https://doi.org/10.1152/jn.01308.2007.

Lacquaniti, F., Ivanenko, Y.P., Zago, M., 2002. Kinematic control of walking. Arch. Ital. Biol.

Martelli, D., Vannetti, F., Cortese, M., Tropea, P., Giovacchini, F., Micera, S., Monaco, V., Vitiello, N., 2014. The effects on biomechanics of walking and balance recovery in a novel pelvis exoskeleton during zero-torque control. Robotica 32, 1317–1330. https://doi.org/10.1017/S0263574714001568.

Monaco, V., Tropea, P., Aprigliano, F., Martelli, D., Parri, A., Cortese, M., Molino-Lova, R., Vitiello, N., Micera, S., 2017. An ecologically-controlled exoskeleton can improve balance recovery after slippage. Sci. Rep. 7, 46721. https://doi.org/10.1038/srep46721.

Tropea, P., Vitiello, N., Martelli, D., Aprigliano, F., Micera, S., Monaco, V., 2015. Detecting slipping-like perturbations by using adaptive oscillators. Ann. Biomed. Eng. 43, 416–426. https://doi.org/10.1007/s10439-014-1175-5.